ARTICLE IN PRESS

Physica B xx (xxxx) xxxx–xxxx

Contents lists available at ScienceDirect

Physica B

journal homepage: www.elsevier.com/locate/physb

Synthesis of $Y_{1-x}Al_xBa_2Cu_3O_{7-\delta}$ via combustion route: Effects of Al_2O_3 nanoparticles on superconducting properties

Mohd Shahadan Mohd Suan[a,*], Mohd Rafie Johan[b]

[a] Department of Engineering Materials, Faculty of Manufacturing Engineering, Universiti Teknikal Malaysia Melaka, 76100 Durian Tunggal, Melaka, Malaysia

[b] Nanomaterial Engineering Research Group, Advanced Materials Research Laboratory, Department of Mechanical Engineering, University of Malaya, 50603 Kuala Lumpur, Malaysia

ARTICLE INFO

Keywords:
$YBa_2Cu_3O_{7-\delta}$
Al_2O_3 nanoparticles
Magnetic J_C
Combustion synthesis
Pinning effect
Superconducting properties

ABSTRACT

Combustion reaction was used to synthesis Al_2O_3 nanoparticles embedded $Y_{1-x}Al_xBa_2Cu_3O_{7-\delta}$ simultaneously. The effects of Al_2O_3 nanoparticles with nominal molar mass (x_{mol}) of 0.02, 0.04, 0.06, 0.08 and 0.10 towards the critical current density J_C of $Y_{1-x}Al_xBa_2Cu_3O_{7-\delta}$ were verified by magnetic measurement. Resulted XRD patterns revealed that the calcined samples consist of pure Al_2O_3 and $Y_{1-x}Al_xBa_2Cu_3O_{7-\delta}$ phases which had been confirmed by EDX results. The SEM images showed that Al_2O_3 nanoparticles (~10 nm) were distributed in polycrystalline $YBa_2Cu_3O_{7-\delta}$ grains and grain boundaries. The presence of higher concentration of Al_2O_3 nanoparticles has developed Al^{3+} rich spots which diffused within the $YBa_2Cu_3O_{7-\delta}$ superconducting matrix to form $Y_{1-x}Al_xBa_2Cu_3O_{7-\delta}$ and was confirmed by EDX analysis. The samples were electrically superconducting at temperature above 85 K as measured by using standard four-probe technique. The magnetic field (H) dependent magnetization (M), M-H hysteresis loops measured at 77 K for $x_{mol}\leq 0.06$ samples are significantly improved attributed to the increase of trapped fluxes in the samples. Remarkable increase of magnetic J_C (H) in Al_2O_3 nanoparticles added samples compared to the as prepared polycrystalline $YBa_2Cu_3O_{7-\delta}$ sample indicating strong pinning effect. It is suggested that well-distributed Al_2O_3 nanoparticles in the polycrystalline $YBa_2Cu_3O_{7-\delta}$ matrix achieved via auto-combustion reaction has efficiently pin the magnetic vortex. The magnetic J_C was optimized to ~6 kAcm^{-2} in x_{mol}=0.06 sample. On the other hand, insignificant magnetic J_C improvement in $x_{mol}\geq 0.08$ samples is probably resulted from the agglomerated Al_2O_3 nanoparticles in $Y_{1-x}Al_xBa_2Cu_3O_{7-\delta}$ phase.

1. Introduction

The present $YBa_2Cu_3O_{7-\delta}$ [1,2] is a promising superconducting material for many applications above 77 K as it keeps superconductive though infiltrated by magnetic fluxes (below H_{C2}) [3]. However whence the electrical current is passed through, movements of those fluxes (attributed to Lorentz force) [4,5] will destruct the superconductivity of $YBa_2Cu_3O_{7-\delta}$ [6,7] and reduced the J_C. However, low J_C in typical pure crystalline $YBa_2Cu_3O_{7-\delta}$ can significantly be increased by induced of pinning center materials [8]. The highest J_C achieved in such superconductor evidence the effectiveness of pinning center materials as mechanism to trap the fluxes and increase the J_C. Nevertheless, the research on higher J_C of polycrystalline $YBa_2Cu_3O_{7-\delta}$ is essential for superconducting engineering especially in searching for simpler processes with lower cost of superconducting wire fabrication where various elements and impurities were added into polycrystalline $YBa_2Cu_3O_{7-\delta}$ [9]. In that regards, the addition of alumina Al_2O_3 particles into polycrystalline $YBa_2Cu_3O_{7-\delta}$ matrix has attracted much attention to be as effective pinning materials [10,11]. Addition of 0.04 wt% of Al_2O_3 nanoparticles with size > 10 nm were suggested strongly pin the fluxes [10]. On the other hand, Mellekh et al. [11] had proposed that the increment of J_C was due to grain boundary improvement by incorporation of Al^{3+} ions from Al_2O_3 particles into $YBa_2Cu_3O_{7-\delta}$ structure. Since there were two mechanisms on increasing J_C, the role offered by Al_2O_3 nanoparticles as pinning center material in polycrystalline $YBa_2Cu_3O_{7-\delta}$ need to be optimized. In this light, the citrate-nitrate auto-combustion method [12–14] makes it possible producing of pure Al_2O_3 or $Y_{1-x}Al_xBa_2Cu_3O_{7-\delta}$ polycrystalline samples individually and simultaneously. Besides, this method was capable to synthesis the composite of two distinct phases with homogeneous mixing [15–17] in nanoscale which unable to be achieved using conventional solid state reactions. Therefore in this work, a citrate-nitrate auto-combustion reaction to synthesis well-distributed of Al_2O_3 nanoparticles in pure $YBa_2Cu_3O_{7-\delta}$ samples was presented. The effects

* Corresponding author.
E-mail address: mohdshahadan@utem.edu.my (M.S. Mohd Suan).

http://dx.doi.org/10.1016/j.physb.2016.11.020
Received 30 June 2016; Received in revised form 15 November 2016; Accepted 16 November 2016
Available online xxxx

Please cite this article as: Mohd Suan, M.S., Physica B (2016), http://dx.doi.org/10.1016/j.physb.2016.11.020

of Al_2O_3 nanoparticles towards the magnetic J_C of the polycrystalline $Y_{1-x}Al_xBa_2Cu_3O_{7-\delta}$ samples were elucidated.

2. Experimental

Yittrium Y, Barium Ba, Copper Cu and Aluminum Al nitrate solution with various concentration (0.5, 0.5, 0.25 and 0.5 M) were prepared by dissolving 99.9% pure $Y(NO_3)_3{\cdot}6H_2O$, $Ba(NO_3)_2$, $Cu(NO_3)_2{\cdot}4H_2O$ and $Al(NO_3)_3$ analytical grade reagent into distilled water. The solutions were mixed at mole ratio of Y:Ba:Cu:Al=1:2:3:x where x in a range of 0–0.10. Then citric acid was added to the mixture while the pH of mixture was adjusted to 7.0 by adding ammonia solution. The mixture was heated to 250 °C on the hot plate and put it under infra-red radiation, to achieve a uniform heating. This process has gradually transformed the solution into gel then automatically combusted to form a very fine and reactive ashes. The ashes were calcined in the furnace at 900 °C for 1 h under normal atmosphere to yield stable black powder. The obtained powders were pelletized into 10 mm diameter×2 mm of thickness disks by applying 12.4 MPa load. Then, these pellets were sintered at 960 °C for 1 h under normal atmosphere and soaked at 500 °C in the oxygen flow (50 ml min^{-1}) for 20 h before self-cooling to room temperature. The crystal structure, phase purity of the resulting powders was examined by powder X-ray diffraction (XRD; Rigaku RINT2500Ultra18) using CuKa radiation. Lattice constants were roughly refined by Rietveld method using the Rietan-FP code [18]. The microstructure of the samples was observed at 20,000× magnification using Zeiss Ultra 40XB with EDX spectra capability. For the magnetic J_C measurement, the pellets were cut into rectangular bar with dimension of 1 mm×1 mm×4 mm using diamond cutter. Then, the magnetic flux (μ_0H) with the strength of −1 T to 1 T cycle was applied to the sample at 77 K using superconducting quantum interference magnetometer (Quantum Design Co. LTD; MPMS-XL). The extended Bean's model [19]; J_C=20 $\Delta M(H)/(a(1-a/3b))$ was used to determine the magnetic J_C from the hysteresis curve where ΔM is the vertical width of the magnetization hysteresis (emu cm^{-3}), a and b (cm) are the cross-sectional dimensions of the sample perpendicular to the applied field with b≥a.

3. Results and discussion

Fig. 1 shows the XRD patterns for pure $YBa_2Cu_3O_{7-\delta}$ and Al_2O_3 added $Y_{1-x}Al_xBa_2Cu_3O_{7-\delta}$ samples. Each XRD pattern was identical with significant peaks occurred for polycrystalline $YBa_2Cu_3O_{7-\delta}$ as most dominant structure. The intensity differences of XRD peaks were attributed from the alteration of the structural parameters of the samples. The lattice parameters obtained from the XRD refinement using Rietveld analysis as revealed in the previous work [20] was listed in Table 1. The lattice constants of the samples were consistent with orthorhombic structure of $YBa_2Cu_3O_{7-\delta}$. The lattice parameters of samples x_{mol}≤0.06 were slightly change because Al_2O_3 phase was believed to exist as distinct phase and well dispersed in the $YBa_2Cu_3O_{7-\delta}$. While the abrupt changes of a and c in x_{mol}≥0.08 samples can be attributed from the oxygen deficiencies and Al^{3+} may try to fit in the Y site to form $Y_{1-x}Al_xBa_2Cu_3O_{7-\delta}$. At the sintering temperature, Al^{3+} ions could be possibly incorporated into the $YBa_2Cu_3O_{7-\delta}$ structure to partially replace Y^{3+} ion and thus resulted in the increment of c lattice constant. Upon this point, the oxygen content in $YBa_2Cu_3O_{7-\delta}$ was also re-adjusted to provide stoichiometric balance to the compound. This adjustment resulted in the increment of a lattice constant. Although Al_2O_3 peaks were unable to be detected on the XRD patterns attributed to its lower composition and highly dominant of $YBa_2Cu_3O_{7-\delta}$ peaks, the obtained EDX result [21] listed in Table 1 had confirmed the existence of Al_2O_3 phase.

From the EDX analysis of the grain structure, it was found that the atomic ratio of Y, Ba, and Cu elements for each sample was 1:2:3 which indicate the formation of $YBa_2Cu_3O_{7-\delta}$ phase. This spectra was consisted of very low fraction of Al (below 1%) for samples with x_{mol}≥0.08 attributed to the diffusion of Al into the $YBa_2Cu_3O_{7-\delta}$ structure. This is in agreement with the XRD results for these compositions, where the c lattice parameter of $YBa_2Cu_3O_{7-\delta}$ was significantly increased. Pointed EDX analysis on nanoparticles provided the evidence of Al_2O_3 existence in each sample. In x_{mol}≤0.06 samples, Al and O were the only elements detected. It was found that the atomic ratio of these elements were consistent with the atomic formula of Al_2O_3 phase. Hence, it proved that Al_2O_3 nanoparticles were successfully synthesized and distributed in these samples. While in x_{mol}≥0.08 samples, other elements including Y, Ba, and Cu has been detected together with Al and O. Existence of these elements may be attributed to molten $YBa_2Cu_3O_{7-\delta}$ phase which had covered the Al_2O_3 nanoparticles.

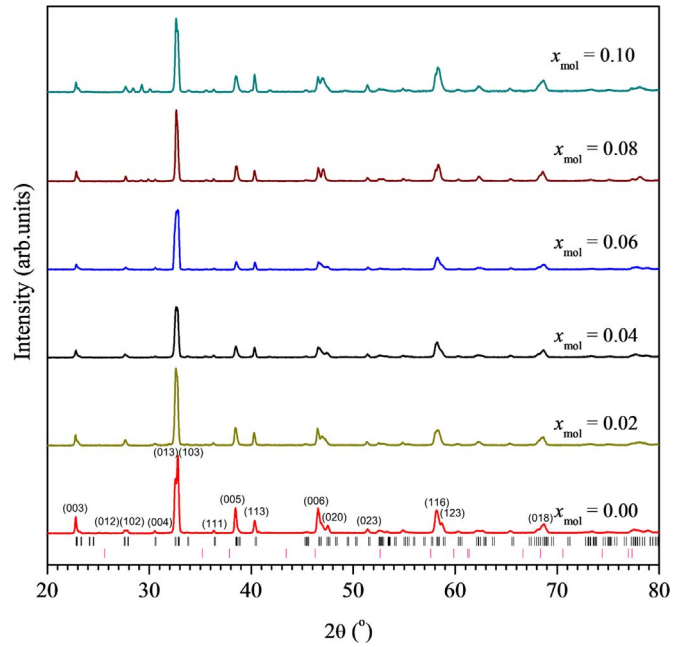

Fig. 1. XRD pattern of $YBa_2Cu_3O_{7-\delta}$ and Al_2O_3 nanoparticles added $Y_{1-x}Al_xBa_2Cu_3O_{7-\delta}$ samples. Bars at bottom indicated Bragg diffraction pattern for $YBa_2Cu_3O_{7-\delta}$ and Al_2O_3 respectively.

Fig. 2 shows the microstructure of x_{mol}=0.00, 0.06, and 0.10 samples. It was observed that the $YBa_2Cu_3O_{7-\delta}$ was yielded as polycrystalline structure with average particle size of 50 nm (Fig. 2(a)). Additions of Al_2O_3 into $YBa_2Cu_3O_{7-\delta}$ have resulted with existence of two distinct particulate structures as shown in Fig. 2(b). Dispersed nanoparticles with average size of 10 nm was determined as Al_2O_3 while the bigger structure is $YBa_2Cu_3O_{7-\delta}$. The Al_2O_3 nanoparticles of this composition was more likely acted as reinforcing particle rather than incorporate in $YBa_2Cu_3O_{7-\delta}$ structure. The same microstructure was occurred in x_{mol}=0.02 and 0.04 samples. While the x_{mol}=0.10 sample was observed to have molten-like and dense microstructure. It was estimated that $YBa_2Cu_3O_{7-\delta}$ particles have the size ranged from 200 to 400 nm which consisted of many grains. The Al_2O_3 nanoparticles (~10 nm) of this sample were agglomerated at labeled region on Fig. 2(c). At higher addition of Al_2O_3 nanoparticles such in samples with x_{mol}=0.08 and 0.10, sort of melting was occurred at $YBa_2Cu_3O_{7-\delta}$ inter-particles. Al_2O_3 nanoparticles which instead to be distributed within the grains were agglomerated at the grain boundaries of $YBa_2Cu_3O_{7-\delta}$. Agglomeration of Al_2O_3 nanoparticles developed regions with high density of Al^{3+} which were diffused into the $YBa_2Cu_3O_{7-\delta}$ structure hence replaced a fraction of Y^{3+} site. The replacement is visible in EDX analysis, as higher amount of Al was detected in $YBa_2Cu_3O_{7-\delta}$ as well as Y at Al_2O_3 nanoparticles.

Fig. 3 shows the T_C onset and T_C zero of the samples. It was observed that both T_Cs were decreased with increasing the content of